Global Journals LaTeX JournalKaleidoscope™
Artificial Intelligence formulated this projection for compatibility purposes from the original article published at Global Journals. However, this technology is currently in beta. *Therefore, kindly ignore odd layouts, missed formulae, text, tables, or figures.*

Finite Element Simulation of the Reverse Bending and Straightening of Steel Bars Used For Civil Engineering Applications

Adewole[1]

[1] Newcastle University

Received: 11 June 2012 Accepted: 3 July 2012 Published: 15 July 2012

Abstract

Steel bars used for pre-stressing concrete and as tensile armour wires are routinely subjected to reverse bending and straightening test to detect laminations in the bars. In this paper, three dimensional FE simulation of the reverse bending and straightening of steel wires over rotating rollers conducted as a part of the research to numerically investigate the effects of the combination of reverse bending and laminations on the tensile properties of bars for civil engineering applications is presented. The appropriateness of the simulation procedure employed in this work is demonstrated by a good agreement between the finite element and experimental results.

Index terms— steel bars, FE simulation, Reverse bending and straightening test, Static roller, Tensile armour wire.

1 Introduction

arbon steel bars are steel elements/materials with sizes from 10mm to 32mm [1]. They are used as pre-stressing steel bars and as flexible pipe tensile armour bars which provides longitudinal and hoop (circumferential) tensile stress resistances for flexible pipes used for offshore oil and gas transportation. Carbon steel bars are subjected to routine reverse bending and straightening test which involves bending the bars over a rotating left hand roller, reverse bending the bars over the middle roller and finally straightening of the bars over the right hand roller as shown in Figure **??** to detect laminations in bars. Laminations (particularly the type that may be present in carbon steel bars used for civil engineering application) are line type defects or long cracks which are normally invisible at the surface, are generally parallel to the rolling or drawing direction and are usually revealed through reverse bending of the bars [2]. Crack-like laminations (longitudinal cracks) have been found to be instrumental to the fractures of the pre-stressing wires (carbon steel elements/materials smaller than bars with sizes from 2.5mm to 8mm) of ruptured pre-stressed concrete pipe [3].

Most of the published literature on bending and reverse bending of metal products such as the work of [4][5][6][7], among others, relates to the processing of sheet metal during sheet metal forming operations. The few literature that deals with the bending and reverse bending of wires includes the experimental work conducted by [8] on reverse bending for descaling of wire rods and the experimental and FE simulation works conducted by [9,10] on the effect of excessive bending, which Aluminium Conductor Composite Core (ACCC) experiences due to the reeling of the wires on mandrels on the axial compressive stress and the residual tensile strength of the wires. To date, neither the FE simulation of the reverse bending, nor the FE simulation of the reverse bending and straightening of carbon steel bars used for civil engineering application has been published.

Figure **??** : Industrial reverse bending equipment with three rollers Author : Newcastle University, Newcastle upon Tyne, United Kingdom, NE1 7RU. E-mail : k.k.adewole@yahoo.com pinning the nodes on the end of the ACCC wire that are in contact with a static mandrel at the beginning of the simulation and applied a concentrated load to the free end of the wire to bend the wire round the mandrel. Although this methodology may produce the

desired bending effects in the wire, it does not simulate the actual bending process in practice. In practice, the mandrel is rotated and the wire is bent and wrapped round the rotating mandrel. Also this modelling approach of bending the wire round a static mandrel instead of the rotating mandrel bending the wire round it could not be used to simulate the reverse bending of wires over the second roller without having to unwind the bent wire from the first roller, thereby introducing the unwinding process which is not part of the reverse bending process in practice. Consequently, this modelling approach could not be used to simulate the reverse bending and straightening of bars used for civil engineering applications.

This paper presents three dimensional FE simulation of the reverse bending and straightening of steel bars used for civil engineering application which was conducted as a part of the research to numerically predict the effects of the combination of reverse bending and straightening process and defects such as laminations and scratches on the tensile properties of the bars. Numerical prediction methodology was employed in the research because it was not possible to machine the longitudinal line-type or crack-like laminations that are parallel to the bar's length (rolling direction) and cut across the width of the wire experimentally. The reverse bent and straightened (RBS) specimen and the unbent bar specimen were subjected to a tensile testing simulation to determine the effect of the reverse bending and straightening process on the bar in terms of the force-displacement response. The force-displacement curves from the FE simulation of the tensile testing of the RBS and unbent bar specimens were then validated with the force-displacement curves from the laboratory tensile testing of unbent and experimentally RBS bar specimens. The FE simulation was conducted using the combined hardening plasticity models combined with the phenomenological shear failure model in-built in the Abaqus v 6.9.3 material library which has been identified by [11] as an appropriate fracture model for the prediction of the fracture behaviour of the bar considered in this work. The calibrated shear damage and fracture modelling parameters used for the FE simulations are fracture strain of 0.3451, Shear stress ratio of 12.5, Strain rate of 0.000125s -1 and a material parameter Ks of 0.3. Interested readers are referred to Adewole, et al [11] for the details of the shear damage and fracture model and the phenomenological fitting procedure employed to obtain the calibrated shear failure modelling parameter values. The details of the combined hardening plasticity model are presented in section 1.1.

2 a) Combined Hardening Plasticity Model

The combined hardening plasticity model used for this simulation is a combination of the nonlinear kinematic and isotropic hardening models. The isotropic cyclic hardening component is based on the exponential law given in equation (1) obtained from [12]. The kinematic hardening component is based on the evolution of the backstress (a nonlinear evolution of the centre of the yield surface) ? ? given in equation (2) obtained from [12].) 1 (0 pl b i e Q Y ? ? ? ? ? + = (1) pl pl C ? ?? ? ? ? ? ? ? ? =) (1 0 ? (2)

Here 0 ? is the size or magnitude of the yield surface (the limit of the elastic range), i Y is the initial yield stress, ? Q is the maximum stress increase in the elastic range, pl ? is the plastic strain, and b is a material parameter that defines the rate at which the maximum size is reached as plastic straining develops.

? is the overall backstress, C and ? are kinematic hardening parameters, which are material parameters that define the initial hardening modulus and the rate at which the hardening modulus decreases with increasing plastic strain respectively [12].

3 II.

4 Experimental And Fe Analysis Procedures

The details of the experimental and FE simulations are presented in this section.

5 a) Laboratory Reverse Bending, Straightening and Tensile Testing of Bars

The reverse bending, straightening and tensile testing of RBS bar specimen was simulated experimentally in the laboratory by winding a length of the flat bar with 12mmx5mm cross-sectional dimension round a 100mm roller as shown in Figure 2. The bent bar length was then reverse bent in the opposite direction over the same 100mm roller. The reverse bent bar length was finally straightened and cut into tensile test specimens. The RBS specimen and the unbent specimen were then subjected to tensile testing using an Instron universal testing machine (IX 4505) fitted with an Instron 2518 series load cell with a maximum static capacity of ±100 kN. The displacement was measured The FE simulation of the bending, reverse bending, straightening and tensile testing of the flat bar was conducted in four simulation steps. Figure 3 shows the arrangement used for the simulation which consists of a 305mm long tensile armour bar strip between the left roller (Roller 1) and the right roller (Roller 2), and a guide plate. The guide plate was introduced to prevent Roller 2 from lifting vertically upward during the bending simulation. The 305mm long bar consist of a 50mm long central tensile testing specimen and two 127.5mm long left and right attachments. The attachments were introduced to prevent localised deformation of the ends of the tensile testing specimen, which occurred when the specimen was bonded to the rollers directly. The whole model was meshed with C3D8R elements (8-node hexahedral linear brick reduced integration elements with hourglass control). The rollers and the guide plate were meshed with 3mmx3mmx3mm elements while the attachments and the specimen were meshed with elements having 3mmx3mmx0.5mm and 3mmx1mmx0.5mm

dimensions respectively. The 1mm dimension is along the specimen length and the 0.5mm dimension is along the specimen thickness, which translates to 10 elements along the bar thickness. The specimen was meshed with the finest mesh in order to obtain accurate results as the tensile testing simulation was carried out on the 50mm long specimen alone. The rollers, the guide plate and the attachments (which were only introduced to prevent localised deformation of the ends of the specimen) were meshed with a coarse mesh to reduce the output file size and computation time.

The bending simulation was conducted by rotating Roller 1 in an anticlockwise direction to wind the bar round Roller 1. The reverse bending simulation was conducted by rotating Roller 1 in a clockwise direction to unwind the bar whilst simultaneously rotating Roller 2 in an anticlockwise direction to reverse bend and wind the bar round Roller 2. The straightening simulation was conducted by rotating Roller 2 in a clockwise direction to unwind the tensile armour bar and pulling Roller 1 longitudinally and vertically simultaneously, until the attachments and test specimen were straightened. The simulation of the tensile testing of the RBS bar specimen model was conducted on the model of the bar specimen within the rollers-attachmentsspecimen assembly. In order to establish the appropriate boundary conditions to be used for the simulation of the tensile testing of the RBS bar specimen within the rollers-attachments-specimen assembly, tensile testing simulations were conducted on the model of an unbent bar within the rollers-attachments-specimen assembly. The left hand end of the specimen, the left roller and the left attachment were fixed, while the right hand end of the specimen, the right roller and the right attachment, which were free to move only in hand end of the specimen alone was fixed, whiles the right hand end of the specimen alone, which was free to move only in the tensile load direction, was subjected to a longitudinal axial tensile displacement in the tensile load direction as shown in Figure 4. A good agreement between the results of the tensile testing simulation conducted with the unbent bar specimen within the rollers-attachments-specimen assembly and the unbent bar specimen alone was then established as presented later in sections 3.2 and 4. The same simulation boundary conditions applied to the tensile testing of the unbent bar specimen within the rollers-attachmentsspecimen assembly was then applied to the tensile testing simulation of the RBS bar specimens within the rollers-attachments-specimen assembly.

6 Results

The results in terms of the deformed shapes showing the stress and strain distributions at the various stages of the bending, reverse bending, straightening and tensile testing process simulations are presented in this section. All the force-displacement curves in this paper are normalised with experimental ultimate load and displacement at fracture. a) Bending, Reverse bending and straightening simulation results

The deformed shape of the entire 305mm long bar strip showing the longitudinal axial stress (designated as S11 in the contour plot) distribution in the bar and the position of the 50mm gauge length tensile test specimen after the bending simulation, during the reverse bending simulation, after the reverse bending simulation and after the straightening process simulations are shown in Figures 5(a The fracture shapes predicted by the simulations conducted with the unbent bar specimen within the rollers-attachments-specimen assembly and with the unbent bar specimen alone are shown in Figures 9 and 10 respectively. The deformed shape of the entire 305mm long bar showing the longitudinal axial stress distribution in the bar and the fractured RBS tensile test specimen within the rollers-attachments-specimen assembly after the tensile testing simulation is shown in Figure **??**1. The fractured shape of the numerically simulated RBS specimen subjected to tensile testing simulation is shown in Figure 12(a) and the fractured experimentally RBS tensile specimen subjected to laboratory tensile testing is shown in Figure 12(b). The normalised force-displacement curves obtained from the simulations of the tensile testing of the unbent bar specimen alone and the unbent bar specimen within the rollers-attachments-specimen assembly are shown in Figure 13. The normalised force-displacement curves obtained from the simulation of the tensile testing of the numerically simulated RBS specimen and the laboratory tensile testing of the experimentally RBS tensile specimen are shown in Figure 14. IV.

7 Discussion

As shown in Figure 5(b), after the bending simulation, the upper and the lower parts of the bar specimen are subjected to tensile and compressive axial stresses respectively, which agrees with the stress pattern in a bent bars stated by [8]. The tensile and compressive axial stresses caused plastic deformations of the upper and the lower parts of the bar specimen as shown by the equivalent plastic strains in the specimen in Figure 5(c). The middle 20% (approximately two element layers) of the bar specimen's thickness, where the neutral axis lies remains elastic with zero equivalent plastic strain as shown in Figure 5(c). The peak stress and strain occurred at the surfaces of the bar specimen, which agrees with what is reported by [13] and further shows the accuracy of the bending simulation. The peak stress and strain occurred at the surfaces of the bar Substituting the bar thickness, T , of 5mm and the roller diameter, r D , of 100mm in equation (3) obtained from [8] as shown in equation 4 gives a maximum strain, e , of 0.048. The maximum strain of 0.043 predicted by the bending simulation as shown in the equivalent strain contour plot in Figure 5(c) agrees well with the maximum strain value of 0.048 calculated with the analytical expression. This further demonstrates the accuracy of the bending simulation. As shown in Figures **??**, 7(a) and 7(b), the initial upper part of the bar is now subjected to compressive stress and the initial lower half is now subjected to tensile stress during and after the reverse bending simulation as a result of

strain/stress reversal associated with the reverse bending operation. The through thickness deformation pattern of the bar specimen after the reverse bending simulation is similar to that predicted by the bending simulation as the upper and the lower parts of the bar specimen were plastically deformed, while the middle 20% of the bar specimen thickness, within which the neutral axis lies remains elastic with zero equivalent plastic strain as shown in Figure **??**(c).

The initial upper part and the initial lower part of the bar specimen at the beginning of the simulation is now the lower part and the upper part of the bar specimen that has undergone bending, reverse bending and straightening (RBS) and are in tension and compression respectively as shown in Figures **??**(b) and (c). From Figure **??**(c), approximately the middle 20% of the bar specimen thickness also remains elastic after the straightening simulation, while the remaining outer portions of the bar specimen have been plastically deformed. The stress and the strain in the RBS specimen at the end of the straightening simulation represent the residual stress and the accumulated plastic strain in the tensile test specimen at the beginning of the tensile testing simulation. Thus, the upper and lower parts of the RBS bar specimen that was subjected to tensile testing simulation had undergone cyclic tensile and compressive plastic deformations, with residual compressive and tensile stresses respectively, while the middle 20% of the thickness of the bar remained elastic. This leaves the RBS bar specimen with an unbalanced residual stress distribution and a non-uniform through thickness deformation.

The fracture shapes shown in Figures 9 and 10, and the force-displacement curves shown in Figures 13 predicted by the simulations conducted with the unbent bar specimen in the rollers-attachments-specimen assembly and the unbent bar specimen alone are in a good agreement. This indicates that the boundary conditions applied to the reels, attachments and specimen during the tensile testing simulation are appropriate as they have negligible impact on the fracture shape and the tensile response of the specimen with a maximum of 0.19% difference between the tensile properties (occurring in the displacement at fracture) predicted by the two simulations. The good agreements in the fracture shapes shown in Figure 12 and in the force-displacement curves shown in Figure 14 predicted by the simulation of the tensile testing of the numerically simulated RBS bar specimen and the curves from the laboratory tensile testing of the experimentally RBS bar specimen shows the accuracy of the bending, reverse bending, straightening and tensile testing simulations.

V.

8 Conclusion

In this paper, the details of the simulation procedures employed for the simulation of the bending and reverse bending of a flat carbon bar used for civil engineering applications as it is conducted in practice, and the straightening and tensile testing simulation processes are presented. It is demonstrated that the bending simulation procedure employed is able to predict a maximum bending strain that agrees with an existing analytical expression. It is also demonstrated that the bending, reverse bending and straightening simulation methodologies employed are appropriate to predict the behaviour of carbon steel wires for civil engineering application subjected to bending, reverse bending and straightening processes. This is evidenced in the good agreement in the fracture shapes and the tensile responses of the experimentally and numerically RBS bar tensile specimens. This paper thus presents a FE simulation procedure which is essential to the research on the numerical prediction of the effect of the combination of reverse bending and straightening process and laminations on the tensile properties of bars used for civil engineering applications.

2 

Figure 1: Figure 2 :

3 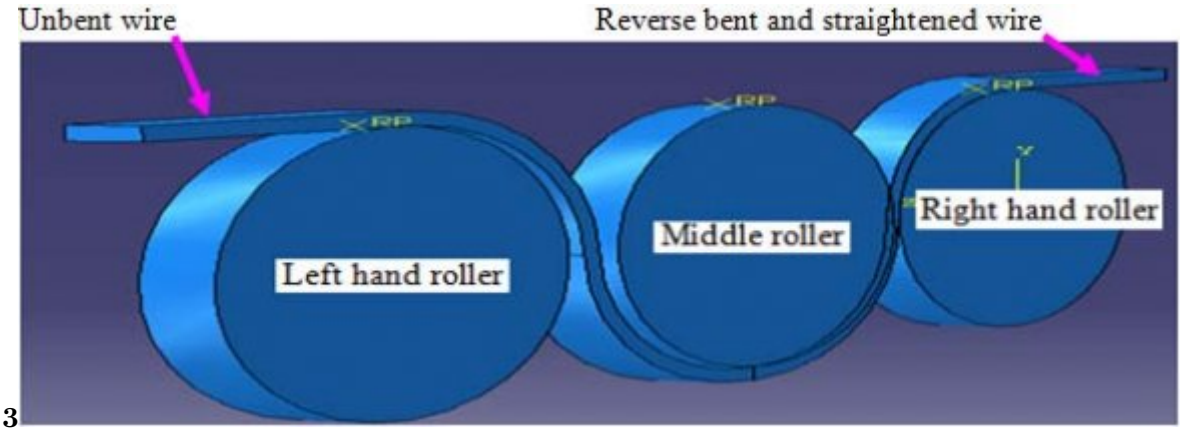

Figure 2: Figure 3 :


4

Figure 3: Figure 4 :

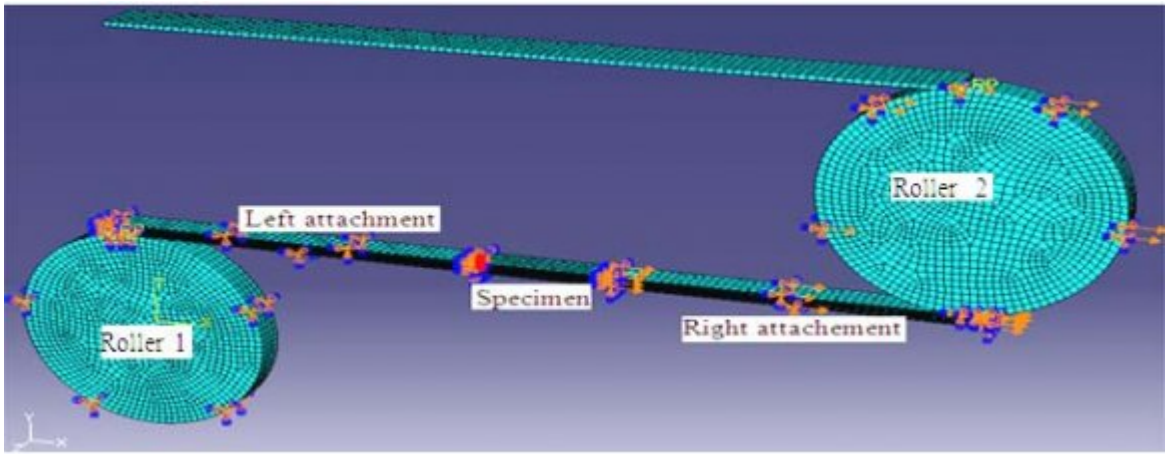

Figure 4:

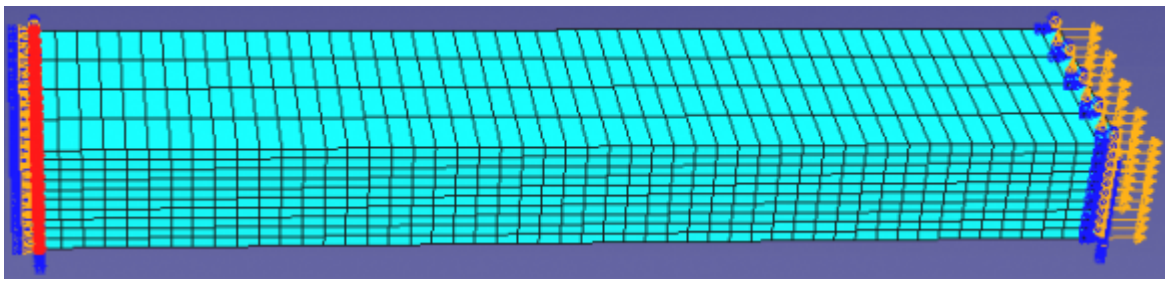

Figure 5:

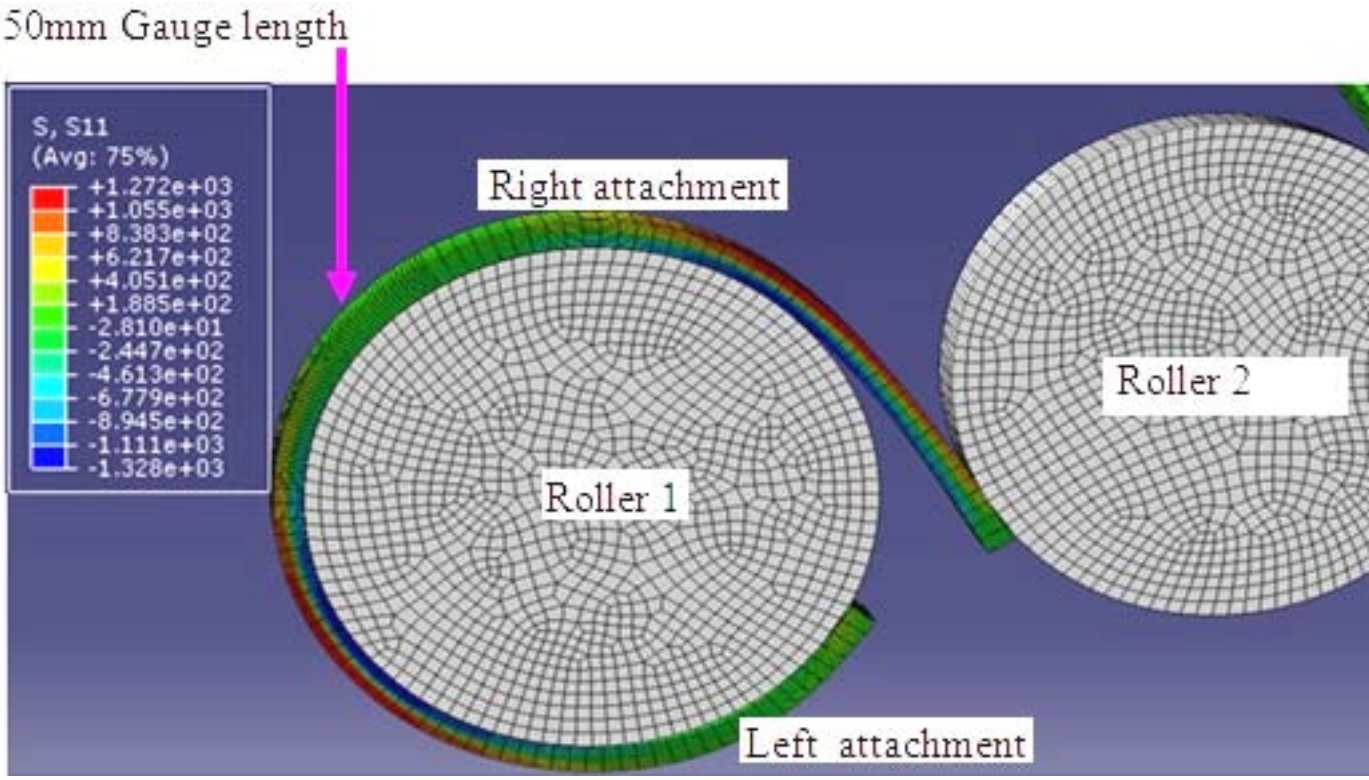

Figure 6: Figure 5 :

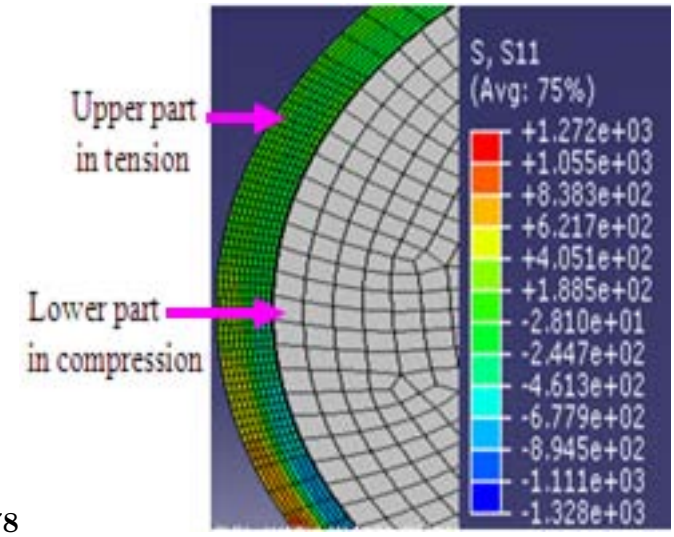

Figure 7: Figure 6 :Figure 7 :Figure 8 :

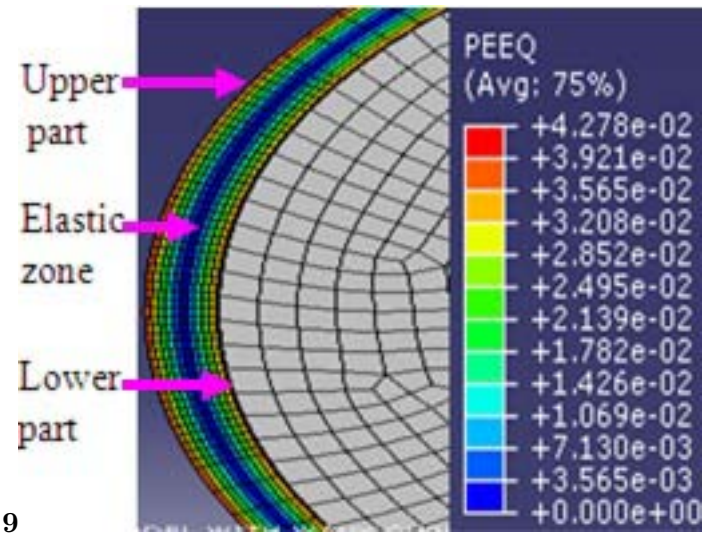

9

Figure 8: Figure 9 :

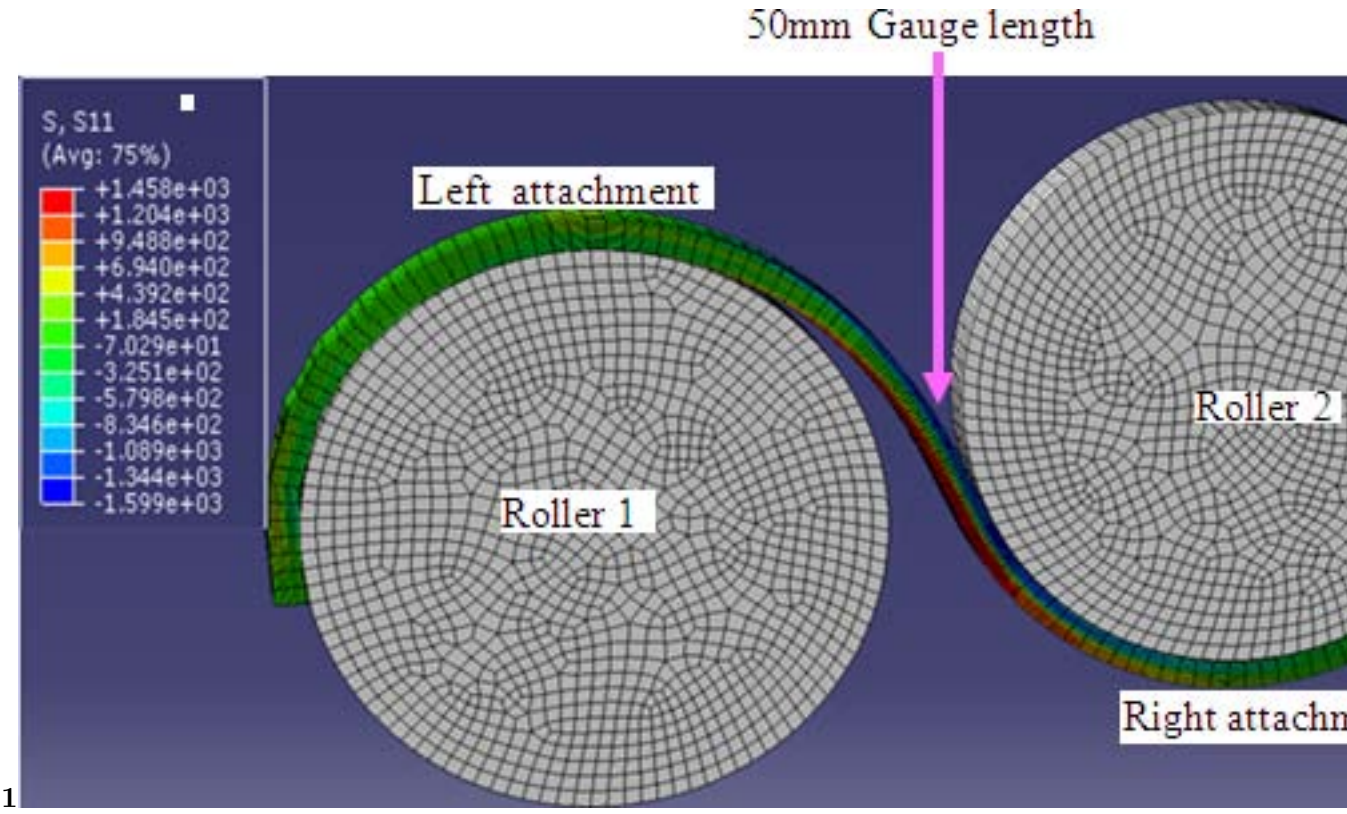

1011

Figure 9: Figure 10 :Figure 11 :

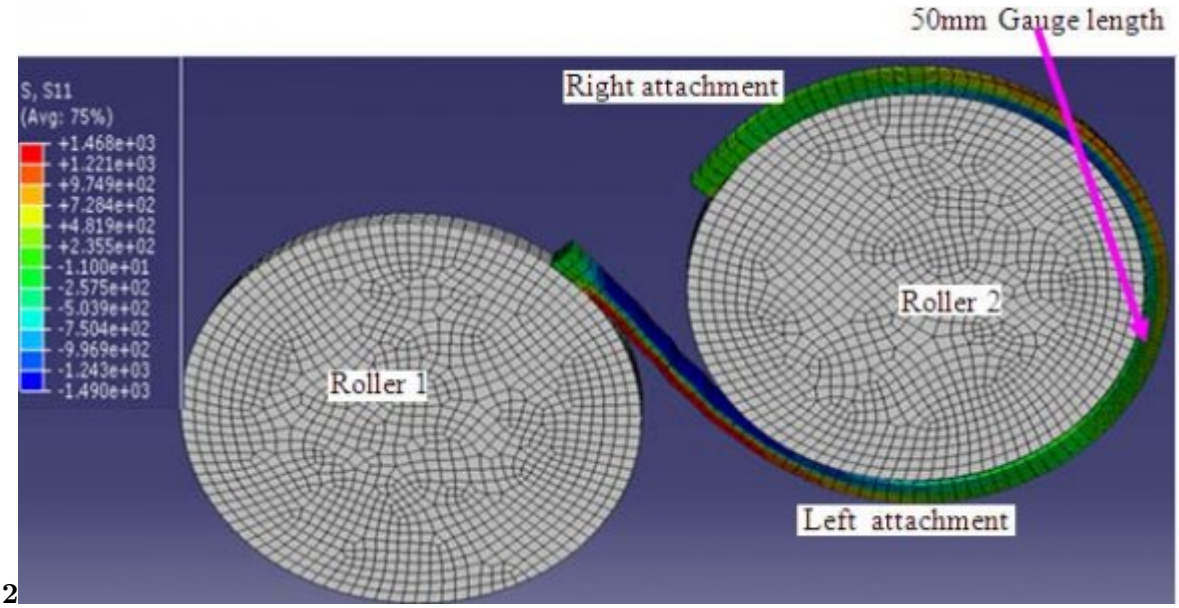

12

Figure 10: Figure 12 :

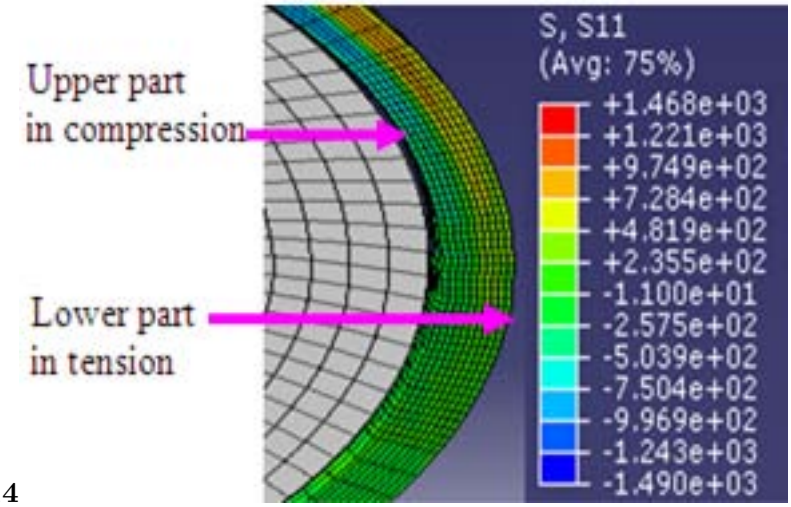

1314

Figure 11: Figure 13 :Figure 14 :

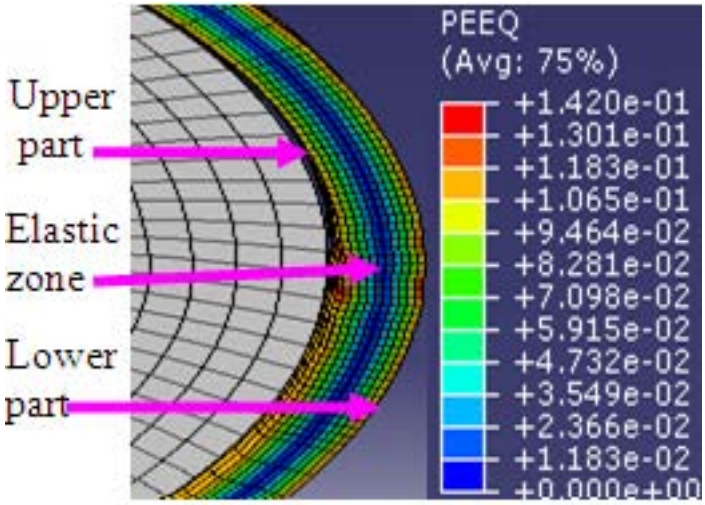

Figure 12: Finite

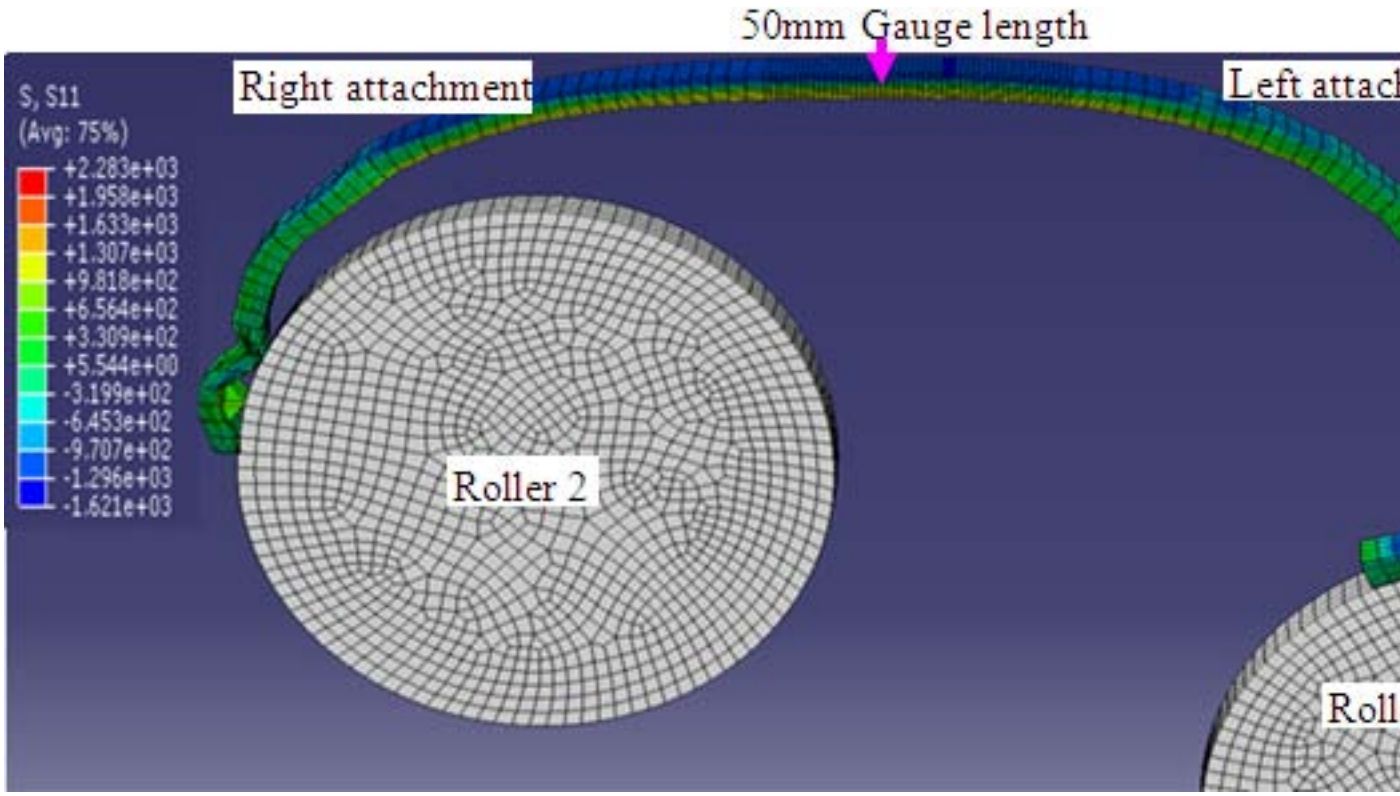

Figure 13:

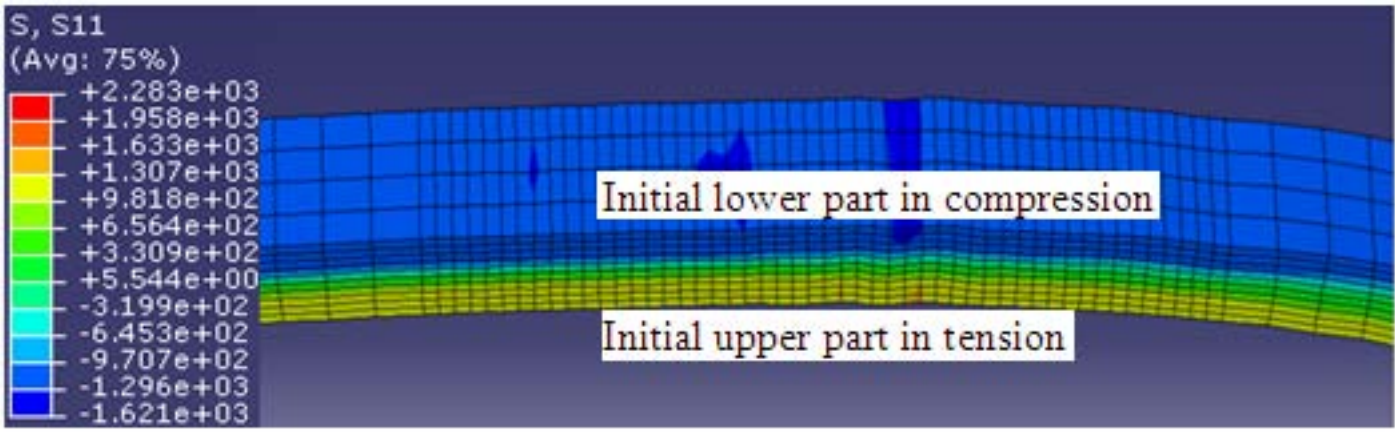

Figure 14:

[Hooputra et al. ()] 'A Comprehensive Failure Model for Crashworthiness Simulation of Aluminium Extrusions'. H Hooputra , H Gese , H Dell , WernerH . *International Journal of Crashworthiness* 2004. 9 (5) p. .

[Gau and Kinzel ()] 'A new model for springback prediction in which the Bauschinger effect is considered'. J T Gau , G L Kinzel . *International Journal of Mechanical Sciences* 2001. 2001. 43 (8) p. .

[Smith et al. ()] *A portable lamination detector for steel sheet, The British Iron and Steel Research Association*, B O Smith , A P Jenning , A G Grimshaw . 1957. Battersea Park Road, London.

[Simulia ()] *Abaqus documentation, Abaqus Incorporated*, Simulia . 2007. (Dassault Systemes)

[Simulia ()] *Abaqus documentation, Abaqus Incorporated*, Simulia . 2007. (Dassault Systemes)

[Carbonnie et al. ()] 'Comparison of the work hardening of metallic sheets in bending-unbending and simple shear'. J Carbonnie , Thuillier , F Sabourin , Brunet , P Y Manach . *International Journal of Mechanical Sciences* 2008. 51 p. .

[Adewole et al. (2011)] 'Determination of the appropriate fracture mechanism for tensile armour wires using micromechanical model-based fracture mechanics'. K K Adewole , Julia M Race , Steve J Bull . *Proceedings of the AES-ATEMA 2011*, (the AES-ATEMA 2011Montreal, Canada) 2011. August 1-5 (2011.

[Tvergaard ()] 'Ductile shear failure at the surface of a bent specimen'. V Tvergaard . *Mechanics of materials* 1987. 6 p. .

[Tvergaard ()] 'Ductile shear failure at the surface of a bent specimen'. V Tvergaard . *Mechanics of materials* 1987. 6 p. .

[Burks et al. ()] 'Effect of excessive bending on residual tensile strength of hybrid composite rods'. B Burks , J Middleton , D Armentrout , M Kumosa . *Composites Science and Technology* 2010. 2010. 70 p. .

[Burks et al. ()] 'Hybrid composite rods subjected to excessive bending loads'. B M Burks , D L Armentrout , M Baldwin , J Buckley , M Kumosa . *Composites Science and Technology* 2009. 2009. p. .

[Gillstrom and Jarl (2006)] 'Mechanical descaling of wire rod using reverse bending and brushing'. P Gillstrom , M Jarl . *Journal of Materials Processing Technology* 2006. 10 March 2006. 172 (3) p. .

[Prestressed Concrete Pipe Failure Jordan Aqueduct, Reach 3 All U.S. Government Documents ()] 'Prestressed Concrete Pipe Failure Jordan Aqueduct, Reach 3'. *All U.S. Government Documents* 1994. United States Bureau of Reclamation (Paper 284. http://digitalcommons.usu.edu/govdocs/284,assess ed on 20/01/2012)

[Sengupta and Menon (2012)] *Prestressed concrete structures*, Almon Sengupta , Devdas Menon . http://nptel.iitm.ac.in/courses/IIT-MADRAS/PreStressed_Concrete_Structures/pdf/1_Introduction/1.2_Advantages_Types%20of%20Prestressing.pdf 09/2012. Madras. Indian Institute of Technology

[Ken-Ichiro ()] 'Simulation of materials processing: theory, methods and applications'. M Ken-Ichiro . *proceedings of the 7th International Conference on Numerical Methods in Industrial Forming Processes–NUMIFORM 2001*, Cedric Xia (ed.) (the 7th International Conference on Numerical Methods in Industrial Forming Processes–NUMIFORM 2001) 2001. p. .

[Firat ()] 'U-channel forming analysis with an emphasis on springback deformation'. M Firat . *Materials and Design* 2007. 28 p. .